Available online at www.sciencedirect.com
SCIENCE DIRECT®
Journal of Pharmaceutical and Biomedical Analysis 39 (2005) 444–454
JOURNAL OF PHARMACEUTICAL AND BIOMEDICAL ANALYSIS
www.elsevier.com/locate/jpba

Solid-state study of mepivacaine hydrochloride

V. Giannellini [a,*], M. Bambagiotti-Alberti [a], G. Bartolucci [a], B. Bruni [b], S.A. Coran [a], F. Costantino [c], M. Di Vaira [b]

[a] *Dipartimento di Scienze Farmaceutiche, Università di Firenze, Via U. Schiff 6, I-50019 Sesto Fiorentino, Firenze, Italia*
[b] *Dipartimento di Chimica, Università di Firenze, Via Della Lastruccia 3, I-50019 Sesto Fiorentino, Firenze, Italia*
[c] *Dipartimento di Chimica, Università di Perugia, Via Elce di sotto 8, I-06124 Perugia, Italia*

Received 10 October 2004; received in revised form 17 March 2005; accepted 18 March 2005
Available online 13 June 2005

Abstract

Different crystalline forms of the local anaesthetic mepivacaine hydrochloride (MH) were revealed by Fourier transform infrared spectroscopy (FT-IR), not by conventional differential scanning calorimetry (DSC). The existence of two polymorphic anhydrous modifications was discovered and further characterized by X-ray powder diffraction and thermal analysis: Form II, the commercial one, and the more stable Form I, obtained by re-crystallization from Form II. Two pseudopolymorphs were also obtained: Form III, a solvate crystallized from ethanol and Form IV, a solvate crystallized from methanol. Single crystal X-ray diffraction data for both solvates were collected and their structures were determined.

Form II, metastable and monotropically related to Form I, generates through desolvation of Form III, very often present in industrial processing, where crystallization from ethanol solution is a common practice. For the sake of clarity, the presence of polymorphic forms should be reported in the drug master files of MH. However, since MH is readily water soluble, the observed polymorphism has no relevance to its typical clinical use as aqueous solutions.

Keywords: Mepivacaine hydrochloride; Polymorphism; Infrared spectroscopy; X-ray diffraction; Thermal analysis

1. Introduction

Pharmaceutical solids can be classified as either crystalline solids, which have regular arrangements of molecules extended in three-dimensions or amorphous solids, which lack the long-range order present in crystals [1,2]. Most marketed pharmaceuticals consist of molecular crystals. Crystalline forms found for a given drug substance are often polymorphs and solvates. Crystalline polymorphs have the same chemical composition, but different crystal structures, and therefore possess different physico-chemical properties. Solvates, also known as pseudopolymorphs, are crystalline solid adducts containing solvent molecules within the crystal structure, in either stoichiometric or non-stoichiometric proportions, giving rise to unique differences in the physical and pharmaceutical properties of the drug. If the incorporated solvent is water, the solvate is termed hydrate. Adducts frequently crystallize more easily than the solvent-free parent species, because of more efficient packing due to the interclosed solvent molecules. A solvate, initially obtained by crystallization, may later transform into the solvent-free form upon drying. Desolvated solvates are less ordered than their crystalline counterparts and are difficult to characterize, because analytical studies indicate that they are unsolvated materials (or anhydrous crystal forms) when, in fact, they may have essentially preserved the structure of the solvated crystal form from which they were derived [2]. Desolvation of crystalline solvates is one of the methods to prepare polymorphs. Various types of phase changes are possible in solid-state hydrated or solvated systems in response to changes in environmental conditions, such as relative humidity, temperature

* Corresponding author. Tel.: +39 055 4573715; fax: +39 055 4573713.
E-mail address: valerio.giannellini@unifi.it (V. Giannellini).

0731-7085/$ – see front matter © 2005 Elsevier B.V. All rights reserved.
doi:10.1016/j.jpba.2005.03.035

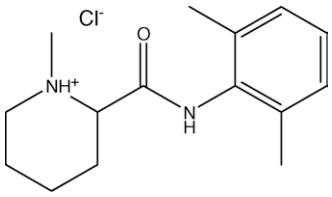

Fig. 1. Mepivacaine hydrochloride (MH).

and pressure. The form obtained may be thermodynamically stable or metastable, which may lead to erroneous interpretations [3].

It is very important to control the crystal form of the drug during the various stages of drug development, because any phase change due to polymorph interconversions, desolvation of solvates, formation of hydrates and change in the degree of crystallinity can alter the bioavailability of the drug. The various effects of pharmaceutical processing on drug polymorphs, solvates and phase transitions have been described in detail by Brittain and Fiese [4].

Various analytical methods are being currently used to characterize the crystalline form of the drug during the various steps of processing and development. The single most valuable piece of information about the crystalline solid, including the existence of polymorphs and solvates, is the molecular and crystalline structure, which is determined by single crystal X-ray diffraction. Powder X-ray diffraction provides a "fingerprint" of the solid phase and may sometimes be used to determine the crystal structure. Once the existence of polymorphism (or solvate formation) is definitely established by single crystal and powder X-ray diffraction, spectral [5] and thermal [3] methods may be employed for further characterization.

Mepivacaine hydrochloride (MH) is a well-established local anaesthetic drug (Fig. 1).

MH is commercialized as the racemate of *S*(+) and *R*(−) enantiomers. The crystal structure of the *S*(+) enantiomer was published some years ago [6]. That study has been recently complemented by a low-temperature structural determination of the *R*(−) enantiomer [7].

Quality controls on some industrial batches showed an IR spectral pattern (Fig. 2, Form I) not identical to the one registered from available standards (Fig. 2, Form II). The FDA original IR pattern [8] was too poorly defined to be useful. Moreover, on the SDBS website [9] a Form I-type spectrum was well readable. Sigma–Aldrich claimed that USP does not require an IR spectrum to validate an MH reference standard, and USP did not release IR spectra. More investigations throughout the literature revealed some confusion about absolute enantiomer configuration [10–13], in spite of unambiguous assignments [6,14]. Accurate and systematic studies on solid-state properties of local anaesthetics are in progress [15], but pertinent MH references date back to 1974 and relate only to thermomicroscopy [16]; a preliminary study on commercial samples suggested the existence of polymorphism and prompted the present investigation.

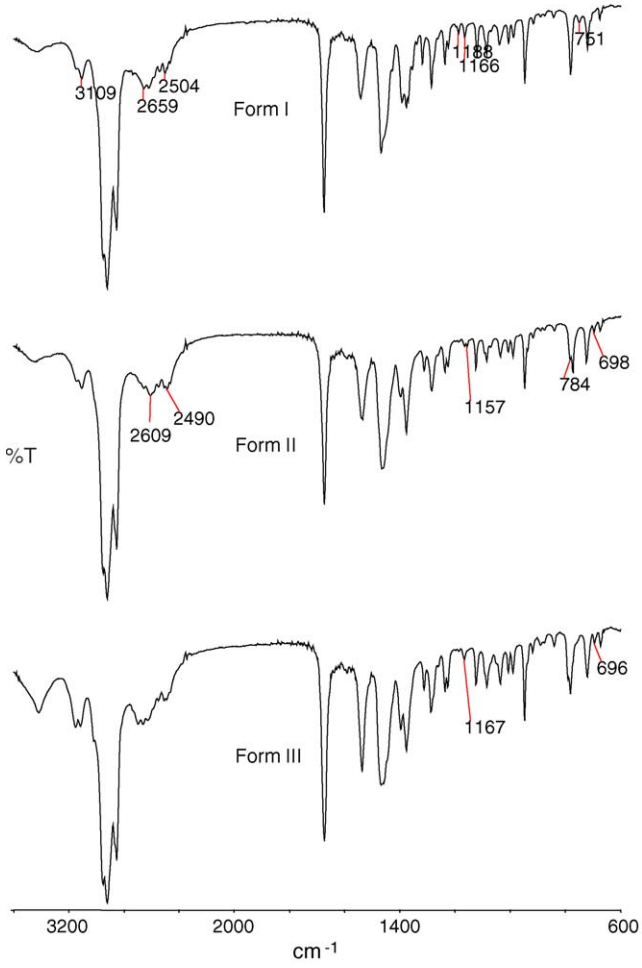

Fig. 2. FT-IR pattern of MH Form I, Form II and Form III (nujol mull).

2. Experimental

2.1. Materials

The basic materials were anhydrous industrial batches (SIMS, Reggello, Firenze, Italia) and USP grade standard (Sigma–Aldrich, Italia) of mepivacaine hydrochloride; they were stored in airtight containers at 4 °C.

Chemical identity of samples was confirmed by NMR, elemental analysis and mass spectrometry. HeadSpace GC–MS analysis proved that all commercial samples were crystallized from ethanol.

MH standard and industrial samples, resulting from extensive grinding or milling, were microcrystalline powders (1–5 μm).

The solvents used were of analytical grade.

2.2. Fourier transform infrared spectroscopy (FT-IR)

Spectra were recorded on a Perkin-Elmer Mod. Spectrum 1000 FT-IR spectrophotometer, equipped with a deuterium triglycine sulfate (DTGS) detector. Setting parameters:

resolution 4 cm^{-1}; apodization weak. The data region was 4000–550 cm^{-1} and the number of scans per spectrum 20. Spectra were obtained in the transmission mode in nujol. Samples were also analysed directly in the attenuated total reflectance (ATR) mode (IR Fourier Transform, Pike Miracle ATR Accessory). Both techniques avoid polymorphic transitions possibly induced by extended grinding and compression to obtain a KBr pellet.

2.3. X-ray single crystal diffraction (XRSCD)

Single crystal X-ray diffraction data for Form III (ethanol solvate, Section 2.6) were collected with a Bruker CCD diffractometer equipped with Goebel mirrors and mounted on a rotating anode generator, using Cu Kα radiation (λ = 1.5418 Å) at room temperature.

Crystal data for Form III: $C_{32}H_{52}Cl_2N_4O_3$, M_W = 611.68, triclinic, space group P, a = 10.562(1) Å, b = 11.646(1) Å, c = 14.343(1) Å, α = 92.79(1)°, β = 96.78(1)°, γ = 102.12(1)°, V = 1708.0(2) $Å^3$, Z = 2, D_c = 1.189 g cm^{-1}, colourless elongated prism, 0.10 mm × 0.30 mm × 0.60 mm, μ = 1.990 mm^{-1}.

The material did not diffract strongly, giving relatively low-angle reflections. An empirical absorption correction was applied with SADABS [17] (0.518–1.000 transmission coefficients range). Of the 5859 reflections measured, 2702 were independent (R_{int} = 0.070) and of these 1153 were "observed" with $I > 2\sigma_I$. The structure was solved by direct methods with SIR [18] and was completed and refined with SHELX-97 [19]. In the final refinement cycles, all non-hydrogen atoms were refined anisotropically and the hydrogen atoms were in calculated positions, riding. The ethanol solvate molecule in disordered position was refined as two complementary images, without geometric constraints. A small damping factor was applied. With 406 parameters, the data/parameters ratio was rather low, as a consequence of rather poor quality of data, but the model is justified by the substantial agreement between the derived structural parameters and expected values (Section 3.2). The final values of the R indices were: R_1 = 0.053 (observed reflections), 0.139 (all data), wR_2 = 0.132. The highest/lowest features in the final ΔF map were 0.15/−0.20 e $Å^{-3}$. ORTEP [20] was used for graphics.

In the search of possible pseudopolymorphs generated by the presence of guest solvate molecules in the lattice, crystals were obtained from MH methanol solutions. These rapidly deteriorated at the air, presumably due to loss of solvate molecules. A quick data collection for cell parameters determination yielded approximate cell-dimensions grossly in agreement with those of Form III, suggesting close similarity in the solid-state structures. However, apparently as a result of a fine energy balance between alternative packing arrangements, different parameters for a unit cell of comparable volume were obtained for a crystal slowly grown in a sealed capillary tube, in presence of the mother liquor. This was used for a relatively low level, but unambiguous, structure determination of Form IV.

Diffraction data for Form IV (methanol solvate) were collected at room temperature with an Oxford Diffraction Xcalibur PX Ultra CCD diffractometer, using Cu Kα radiation.

Crystal data for Form IV: $C_{15.5}H_{25}Cl_1N_2O_{1.5}$, M_W = 298.82, monoclinic, space group $P2_1/n$, a = 8.064(2) Å, b = 21.928(4) Å, c = 9.887(2) Å, β = 106.70(2)°, V = 1674.5(2) $Å^3$, Z = 4, D_c = 1.185 g cm^{-1}, colourless elongated plate, 0.05 mm × 0.20 mm × 0.70 mm, μ = 2.02 mm^{-1}.

The quality of data was affected by the difficult experimental conditions (crystal in capillary with mother liquor and surrounding small crystals). Of the 2935 reflections measured, 892 were independent (R_{int} = 0.117) and of these 447 were "observed" with $I > 2\sigma_I$. The data determination and refinement proceeded as for the Form III model (194 parameters). The methanol solvate molecule, in disordered orientation on an inversion centre, was refined with a geometric constraint on the C–O distance. The final R-values were: R_1 = 0.071 (observed reflections), 0.100 (all data), wR_1 = 0.174 and the highest/lowest features in the final ΔF map were 0.39/−0.30 e $Å^{-3}$.

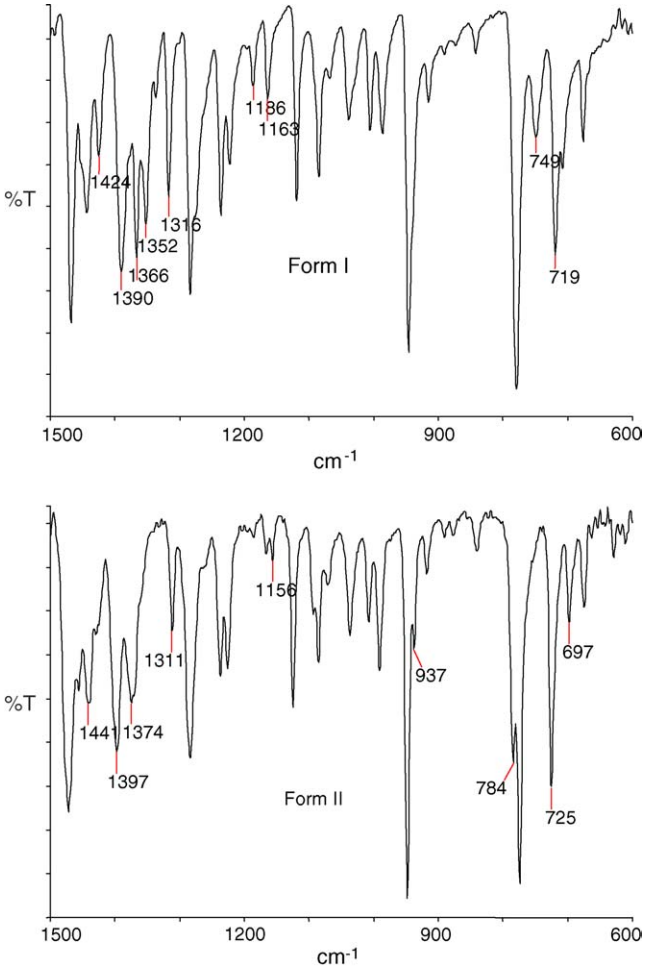

Fig. 3. FT-IR patterns of MH Form I and Form II (ATR mode).

Complete results from the crystallographic analyses on these two structures have been deposited as CIF files with the Cambridge Crystallographic Data Centre, 12 Union Road, Cambridge CB2 1EZ, UK (fax: +44 1223 336033; e-mail: deposit@ccdc.cam.ac.uk) and are available on request quoting the deposition numbers CCDC 266668 (III) and 266669 (IV).

2.4. X-ray powder diffraction (XRPD)

The diffraction patterns were collected using a Bruker D8-Advance powder diffractometer, in θ–θ geometry, using Cu Kα radiation and working at 40 kV and 30 mA. The Sol-X® solid-state Si(Li) detector was used. C/Ni Goebel mirrors in the incident beam were used as monochromator; 1.0 mm divergence and scatter slits and 0.1 mm receiving slit were used.

The diffraction patterns for the simple qualitative analysis were collected in the 3–50° of 2θ range with 1 s/step counting time, while the diffraction patterns for the quantitative phase analysis were collected up to 100° of 2θ and using a larger data collection time (10 s/step).

2.5. Thermal analysis

Differential scanning calorimetry (DSC) analyses were performed with a Mettler TA4000 apparatus equipped with a DSC 25 cell on 5–10 mg samples (Mettler M3 microbalance) scanned in pierced Al pans at 10 °C min^{-1} between 30 and 300 °C under static air.

HyperDSC analyses were performed with a Perkin-Elmer Diamond DSC equipped with Intracooler 3P (−100 °C) on 0.7–1 mg samples scanned in pierced Al pans at 200 °C min^{-1} under N_2 flux.

Coupled thermogravimetric (TG) and differential thermal analysis (DTA) measurements were performed using a Netzsch STA490C thermoanalyser under a 20 mL min^{-1}-air flux with a heating rate of 5 °C min^{-1}.

2.6. Preparation of the samples

Form I, considered to be the most stable one (see below), was crystallized at ambient conditions from a number of solvents, such as water, methanol, acetone, ethanol, methyl ethyl ketone, methylene chloride, *n*-butanol and toluene.

Form II is the form of commercial samples, like the one obtained from Sigma as a standard and most of the industrial batches obtained as a gift from SIMS. Sigma MH USP grade was used as Form II without further purification.

In the course of experiments to obtain Form II from ethanol solutions, attempting to mimic the industrial process, an additional form (Form III) was obtained, characterized and later proved to be a solvate pseudopolymorph. Microcrystals of Form III obtained by rapid re-crystallization (50 °C, under stirring) from an ethanol solution were unstable at the air and underwent a slow transition to Form I (Section 3.3.1). A

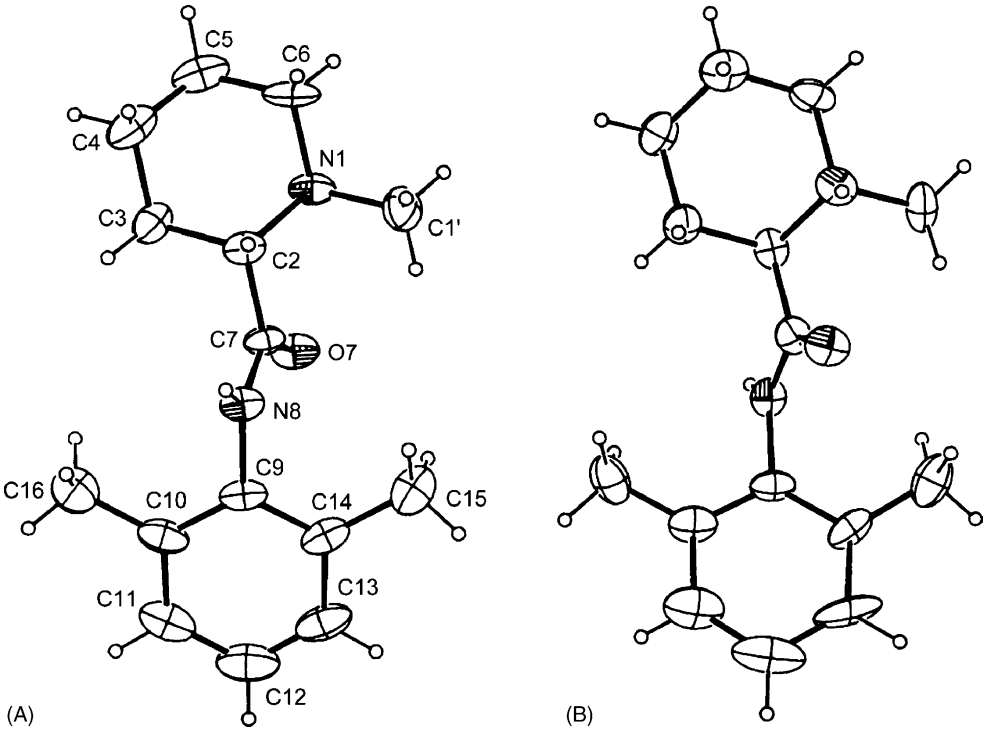

Fig. 4. Views of the two symmetry-independent protonated mepivacaine molecules, denoted molecule A and B, in the structure of Form III. Vibrational ellipsoids are shown at the 20% probability level. Atomic labels, shown only for molecule A, are assigned consistently with the criteria of reference [6]. Geometrical parameters for the two molecules are given in Table 1.

single crystal of Form III, suitable for XRSCD investigation, could be found; its structure was shown (Sections 2.3 and 3.2) to contain half a mole of ethanol per mole MH. A crystal grown from ethanol solution in a sealed capillary tube was also found to belong to Form III, proving that this is the solid phase which exists in equilibrium with the ethanol solution. By the same technique (sealed capillary), a single crystal of methanol solvate was obtained and was shown by XRSCD (Sections 2.3 and 3.2) to contain half a mole of solvent per mole MH, providing an example of a distinct solid phase (Form IV, pseudopolymorph).

Form III was stable in presence of the saturated solution or when separated from the solvent by centrifugation and dried at 50 °C in a vacuum dessiccator; by additional heating at 110 °C for 24 h, a complete transformation to Form II was achieved.

High relative humidity (>80%) converted within a few minutes Form III or Form II to the stable Form I.

Heating Form II at 200 °C for 1 h also caused a complete transformation into Form I.

Form I and Form II were identified by FT-IR and XRPD, which were also used to monitor all phase transformations.

3. Results and discussion

3.1. Fourier transform infrared spectroscopy

The infrared spectrum is very sensitive to the structure and conformation of a compound and can be used to characterize and compare polymorphs.

Fig. 2 reports the FT-IR spectra, recorded in nujol mull, of the USP grade MH standard (Form II), of a sample re-crystallized from ethanol (Form I) and of a sample obtained by rapid re-crystallization from ethanol (Form III).

A spectral pattern pertaining to Form II was also obtained from a MH European Pharmacopoeia standard (kindly provided by Molteni Farmaceutici, Scandicci, Firenze, Italia).

Significant spectral differences between different MH solid phases could be detected. Characteristic bands are evident in the 2700–2450 cm^{-1} and 1600–1300 cm^{-1} regions, and at 1186, 1156, 751 and 697 cm^{-1}.

In Fig. 3, the "fingerprint" regions of the spectra recorded in ATR mode are compared.

FT-IR analyses were performed in attenuated total reflectance to avoid nujol interference and transitions that might take place by grinding for sample preparation, although in the present case no distinctive changes due to transitions after vigorous grinding in a mortar or ball milling were revealed by FT-IR spectra.

Table 1
Bond distances (Å) within the mepivacaine molecule from structural studies

	Form III		Form IV	*S*(+) enantiomer [6]
	Molecule A	Molecule B		
N_1—C'_1	1.492(6)	1.496(6)	1.486(11)	1.491(5)
N_1—C_2	1.497(6)	1.492(6)	1.496(12)	1.499(4)
N_1—C_6	1.495(6)	1.495(6)	1.497(12)	1.506(5)
C_2—C_3	1.509(6)	1.512(6)	1.499(14)	1.515(5)
C_2—C_7	1.517(7)	1.500(8)	1.491(16)	1.522(5)
C_3—C_4	1.510(7)	1.508(7)	1.520(12)	1.528(6)
C_4—C_5	1.489(8)	1.515(7)	1.526(13)	1.514(6)
C_5—C_6	1.490(8)	1.502(7)	1.488(14)	1.496(6)
C_7—O_7	1.221(6)	1.211(6)	1.237(14)	1.231(4)
C_7—N_8	1.323(6)	1.339(7)	1.348(13)	1.335(5)
N_8—C_9	1.431(6)	1.449(7)	1.418(15)	1.438(5)
C_9—C_{10}	1.387(8)	1.389(8)	1.431(15)	1.390(5)
C_9—C_{14}	1.398(7)	1.394(8)	1.357(15)	1.394(5)
C_{10}—C_{11}	1.376(8)	1.345(9)	1.390(15)	1.390(6)
C_{10}—C_{16}	1.502(8)	1.505(8)	1.493(15)	1.503(6)
C_{11}—C_{12}	1.388(9)	1.395(11)	1.346(15)	1.385(6)
C_{12}—C_{13}	1.330(9)	1.375(11)	1.384(14)	1.361(6)
C_{13}—C_{14}	1.400(8)	1.354(9)	1.391(14)	1.396(6)
C_{14}—C_{15}	1.519(8)	1.494(8)	1.545(15)	1.504(6)

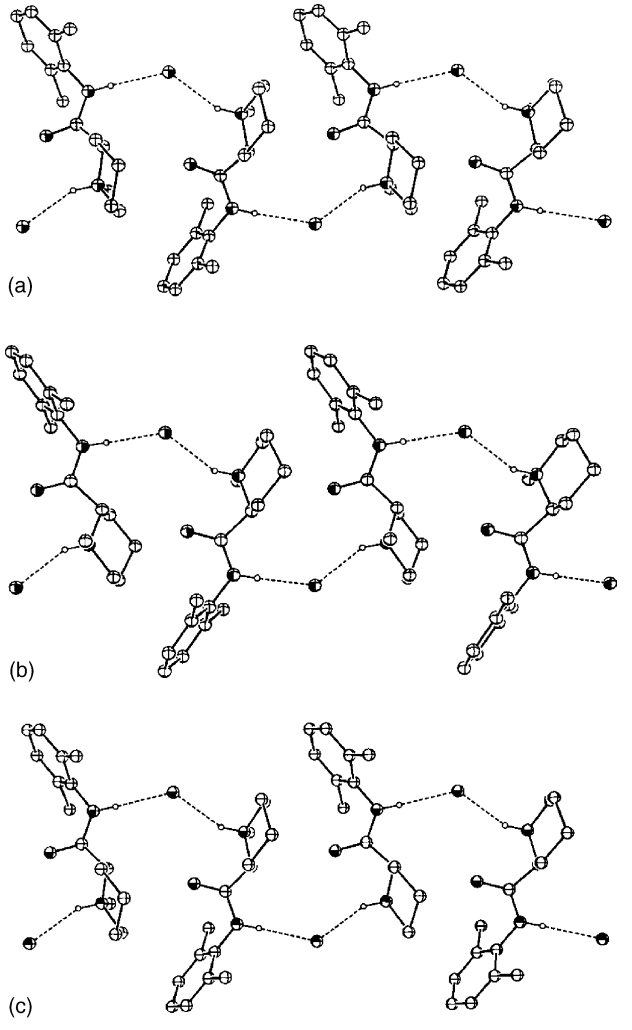

Fig. 5. The one-dimensional pattern of hydrogen-bonded protonated mepivacaine molecules and chloride anions, aligned parallel to the crystallographic a direction in the structure of Form III (a), is compared with the analogous sequence (b) aligned parallel to the b axis in the structure of the *S*(+) enantiomer (reference [6]) and with that (c) along the a–c diagonal in the structure of Form IV.

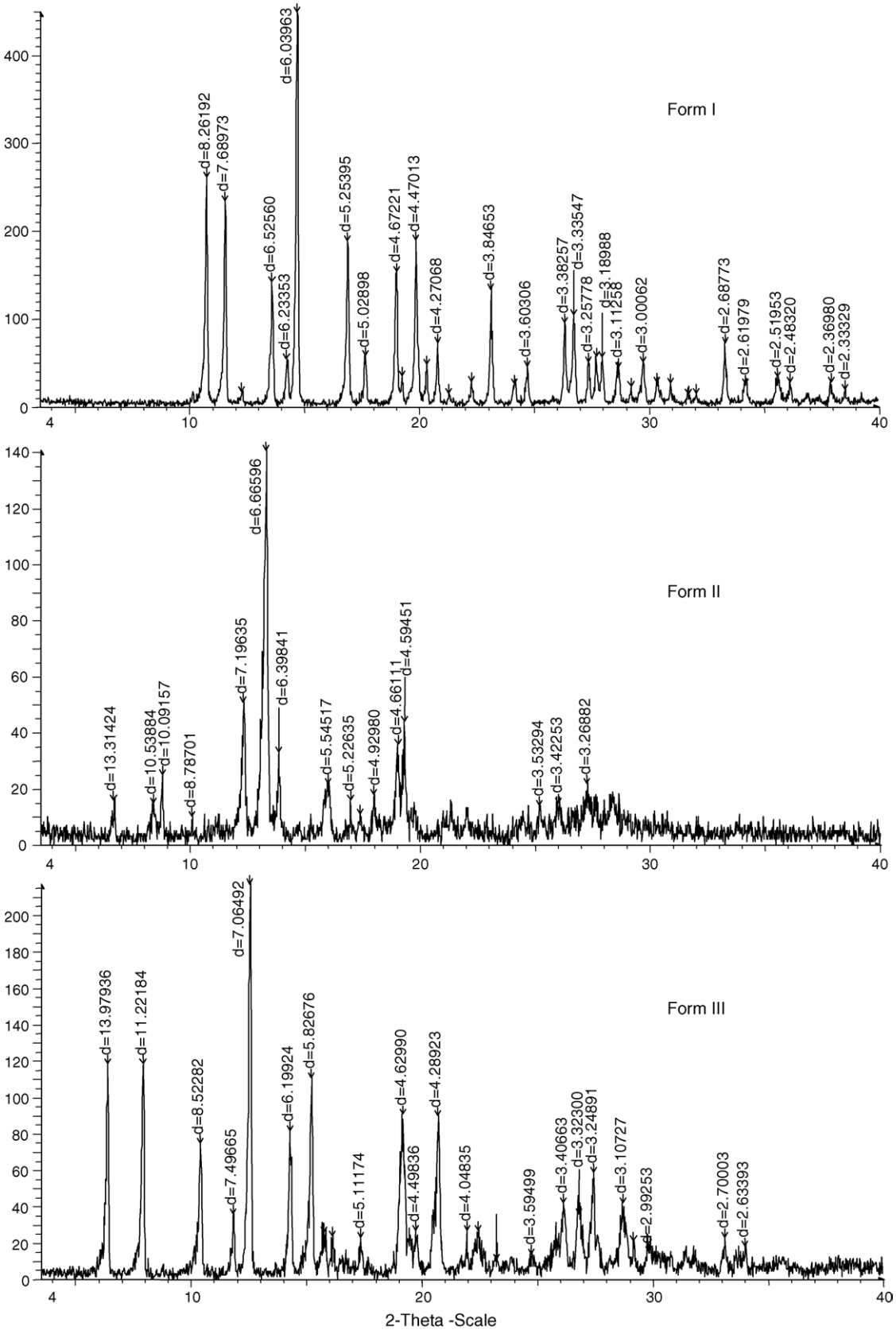

Fig. 6. X-ray powder diffraction patterns of MH Form I, Form II and Form III.

The possibility of minimal sample preparation and the sensitivity to polymorphism make ATR spectrometry an ideal candidate for studies of crystal forms of pharmaceutical compounds. Significant IR spectral differences between the two polymorphs at 696 and 749 cm^{-1} show that ATR FT-IR can provide definitive identification.

3.2. X-ray single crystal diffraction

Full X-ray diffraction studies were performed, as detailed in Section 2.3, on single crystals of Form III and Form IV. On the other hand, single crystals of Form I and Form II, suitable for such investigations, could not be obtained.

The structure of III consists of protonated (at the piperidinium nitrogen) mepivacaine molecules, chloride anions and interposed ethanol molecules. There are four MH units and two solvate molecules in the triclinic unit cell, where the molecule cations are related in pairs by the crystallographic inversion centre, consistently with the presence of a racemic product. The two symmetry-independent cations in the crystallographic asymmetric unit are, in turn, of enantiomeric type with respect to each other (Fig. 4). In the monoclinic unit cell of Form IV, of different shape, but comparable volume to that of Form III (Section 2.3), there are again four MH units and two solvate molecules. The molecule cations belong, in equal numbers, to the two enantiomeric forms, being related by the inversion and reflection operations of the pertaining space group. As shown in Table 1, there is substantial agreement between the geometrical parameters of the two independent molecules in the structure of Form III as well as between these and the room temperature literature values for the *S*(+) enantiomer [6] (or the low-temperature *R*(−) data [7]). Consistent results have also been obtained for the cation of Form IV, in spite of the poor resolution achieved for that structure determination. A remarkable feature, common to all of these structures, is due to the presence of endless chains of alternating mepivacaine (protonated) molecules and hydrogen-bonded chloride ions. The chains are parallel to the crystallographic *a* direction in the structure of Form III, to the *b* direction for the pure enantiomers [6,7] and to a face diagonal for Form IV. As appears from Fig. 5, there are close similarities between these arrangements, in spite of the alternating chirality of cations along the sequences of Form III and Form IV, as opposed to the uniform chirality of the enantiomeric form(s). The crystallographic repeat distances along the chains are comparable for the three cases: 10.562(1) Å (Form III), 10.628(1) Å (room temperature *S*(+) enantiomer's structure [6]) and 10.815(2) Å (Form IV). Moreover, the overall lattice parameters of Form III (Section 2.3) are not very different from those ($a = 9.777(1)$ Å, $b = 10.628(1)$ Å, $c = 15.316(1)$ Å, $V = 1591.4$ $Å^3$) recorded at room temperature for the mepivacaine *S*(+) enantiomer; possibly, the two sets appear to be even closer if, ignoring crystallographic conventions, the labels of the *a* and *b* axes of the orthorhombic enantiomer structure are interchanged to stress similarities in hydrogen-bond trends. In view of this, we suggest that in the course of the slow transformation from Form III to Form I, accompanying the gradual loss of ethanol solvate molecules, the lattice-dimensions of the former approach more and more closely those of an enantiomer's structure. Such an assumption seems to be required in order to rationalize striking similarities between powder diffraction patterns (Section 3.3.1) of these species. The lattice parameter for the direction parallel to the chains of hydrogen-bonded ions

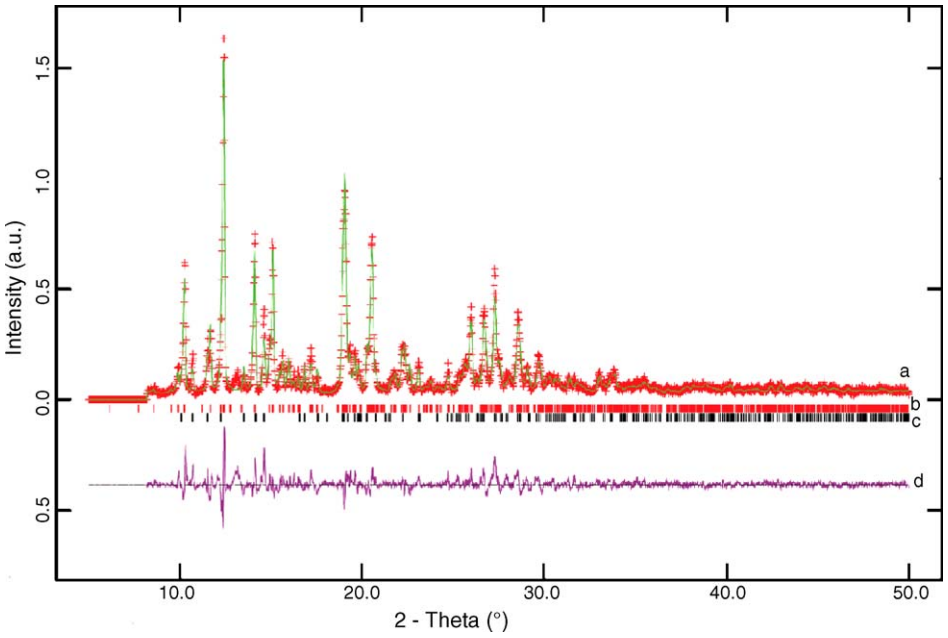

Fig. 7. Rietveld plot for the diffraction pattern 3 (3–50° of 2θ region); observed and calculated (a) and difference (d) curves are shown; (b) sticks = calculated positions of the reflections of Form III; (c) sticks = calculated positions of the reflections of Form I.

appears to be least affected by the above structural change, whereas most of the 7% volume decrease from Form III to Form I (assigning to Form I the cell volume of the room temperature enantiomer structure) is distributed among the other directions. Obviously, the structure of the racemic compound may never fit exactly that of a single enantiomer, but it could approximately do so at the expense of a small amount of disorder, in view of the limited differences between the enantiomeric molecules (Fig. 4).

3.3. X-ray powder diffraction

X-ray powder diffraction is a powerful technique for the identification of crystalline solid phases. Every crystalline solid phase has a unique XRPD pattern, which can form the basis for its identification. The XRPD patterns of the two polymorphs indicate distinct differences in the crystal packing.

In Fig. 6, the XRPD patterns of Form I, Form II and Form III are shown.

3.3.1. Quantitative phase analysis

A set of diffraction patterns of Form III, obtained by rapid re-crystallization (and no additional treatment) from an ethanol solution (Section 2.6), were collected at 15-day intervals on the sample exposed to the air.

A progressive transition from Form III to Form I was observed, eventually leading to complete Form III disappearance. The relative amounts of the two forms present in the diffraction patterns were estimated by the Rietveld method and using the Bish and Howard formula [21] implemented in the GSAS program [22]. The amorphous content was estimated by the internal standard method [23]; microcrystalline Si (200 mesh) was used as a reference standard and it was added to all of the samples in an Si/sample = 1/10 weight fraction ratio.

The amount of the amorphous phase X_a was calculated directly from the weight of the internal standard according to the following equation:

$$X_a = \frac{1}{1 - X_s}\left[1 - \frac{X_s}{X_{s,c}}\right],$$

where X_s is the weight fraction of the internal standard added to the mixture and $X_{s,c}$ is its calculated weight fraction after the Rietveld refinement.

The structural parameters (lattice constants and atomic parameters) for Form I were taken from Csöeregh [6], whereas for Form III those derived from the single crystal analysis were used (Section 2.3).

The profile was modelled using a Pseudo Voigt profile function (six terms) with two terms for the modelling of the asymmetry at low 2θ angle.

The Chebyschev function (14–24 terms) was used for background modelling.

The Gaussian and Lorentzian profile terms, sample displacement and scale factors were refined.

At the end of the refinement, the shifts on all parameters were smaller than their standard deviations. In all cases, no amorphous phase was detected, because the calculated and the experimental weight fraction of internal standard, after the Rietveld refinement, were the same.

Fig. 7 represents the final Rietveld plot for the pattern 3 in the 3–50° of 2θ range after 70 refinement cycles; observed, calculated and difference curves are shown.

Table 2 shows the phase percentages of Form I and Form III in the diffraction patterns recorded at different times.

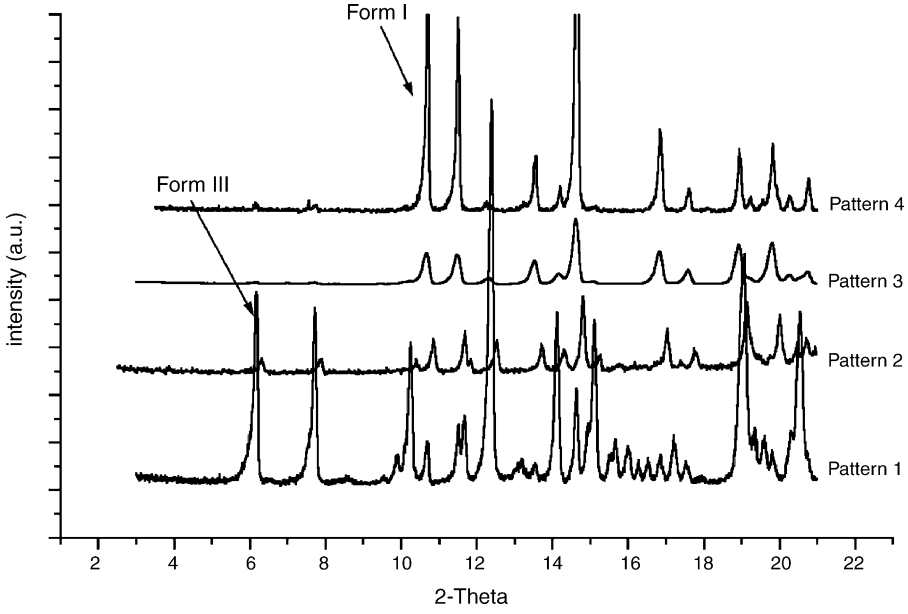

Fig. 8. Phase transition from Form III to Form I.

Table 2
Relative amounts, estimated with the Rietveld method, of Form I and Form III in the diffraction patterns recorded at different times

Pattern	Form I (%)	Form III (%)	Amorphous	*R*-patterns	
1	9.0	91	0	$R_{wp} = 0.16$	$R_p = 0.12$
2	57.5	42.5	0	$R_{wp} = 0.15$	$R_p = 0.11$
3	88.5	11.5	0	$R_{wp} = 0.11$	$R_p = 0.08$
4	100	0	0		

$R_{wp} = \left[\sum w(I_o - I_c)^2 / \sum w I_o^2\right]^{1/2}$; $R_p = \sum |I_o - I_c| / \sum I_o$.

The patterns are compared in Fig. 8: the phase transition is revealed by disappearance of the characteristic peaks of Form III (patterns 1 and 2) and by the appearance of the Form I characteristic peaks (patterns 3 and 4).

3.4. Thermal analysis

Differential scanning calorimetry is a widely applied technique in drug polymorphism studies, but it does not in itself provide sufficient evidence for the existence of polymorphism; it is essential that other techniques be applied to analyse this phenomenon correctly.

The DSC curve at 10 °C min^{-1} of solvate Form III shows two endotherms, the one at 160 °C being due to loss of ethanol (Fig. 9b).

The DSC curve at 10 °C min^{-1} of all MH industrial samples (Form I or Form II) or MH USP grade (Form II) showed only one endotherm of fusion, corresponding to the identical literature melting point, with decomposition (Fig. 9a); identical results were obtained in all experiments from 5 to 50 °C min^{-1}.

A solid-solid phase change may not be revealed by DSC due to its very small transition enthalpy. In these cases, a relatively low-heating rate leads to the total transformation to the high melting form without detecting any transition in the DSC scan. Changes of structure during the heating of the sample, for which no DSC thermal event is detectable, could be clearly demonstrated by temperature-controlled XRPD or FT-IR, if available.

Only HyperDSC experiments at 200 °C min^{-1} discriminated Form I and Form II. In Fig. 10, the traces of the

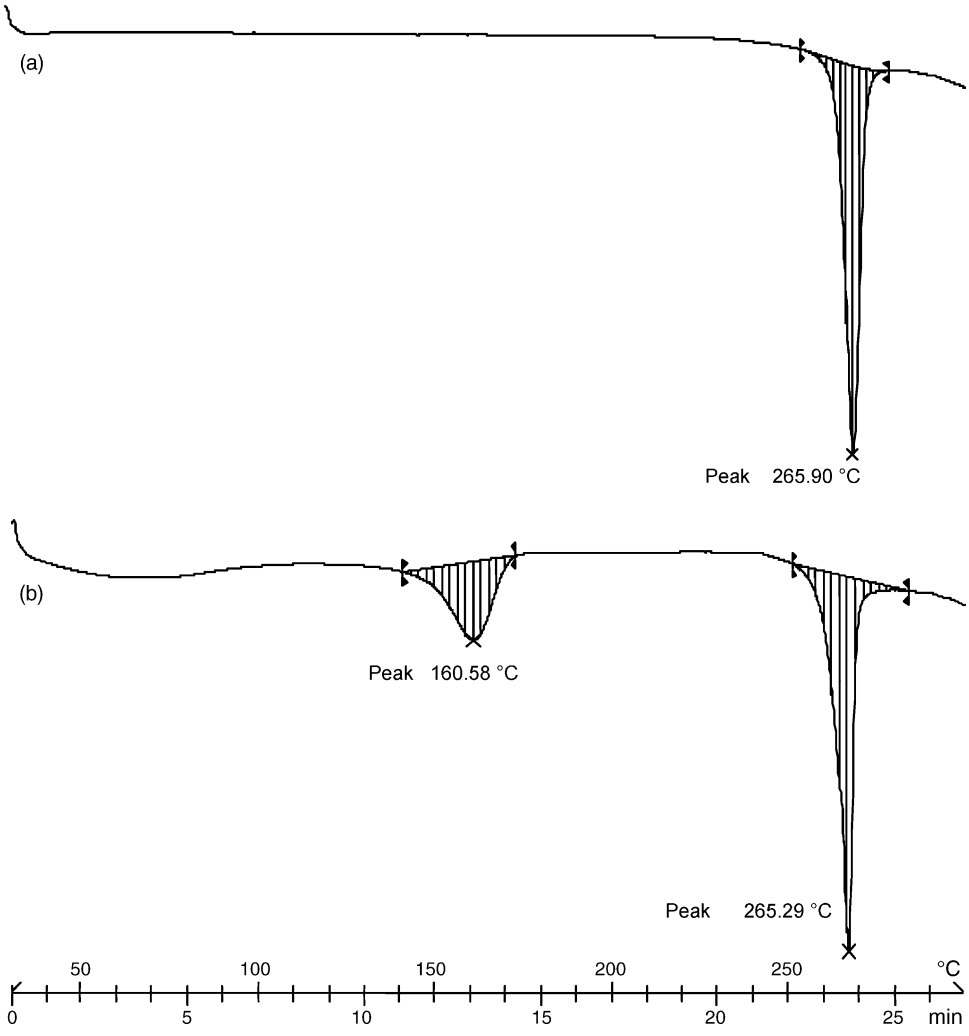

Fig. 9. DSC traces at 10 °C min^{-1} for MH Form I and Form II (a) and Form III (b).

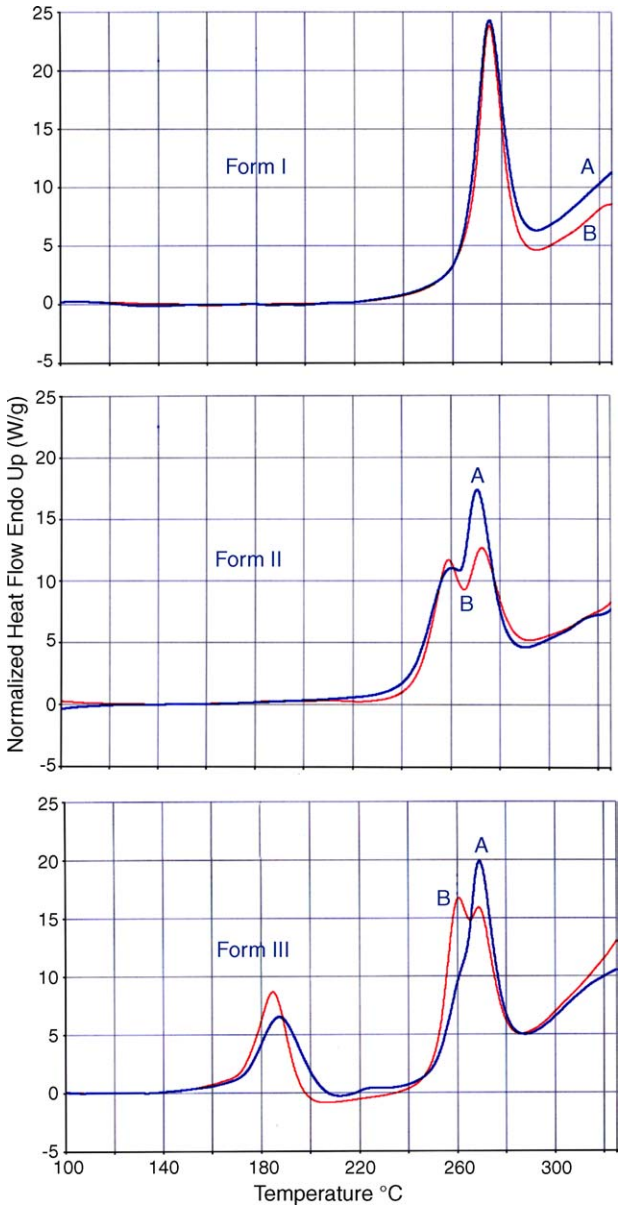

Fig. 10. HyperDSC traces at 200 °C min^{-1} for MH Form I, Form II and Form III. Experiment B was performed 40 days after experiment A, with samples kept in the air at room temperature.

experiments on Form I, Form II and Form III are reported. Melting point values were higher than those of conventional DSC due to the analytical heating rate. In HyperDSC sample, changes that can occur during slow heating of conventional DSC can be eliminated. A quick heating rate allows the melting of the lower melting form to be obtained since the heating rate is faster than phase transition. The B traces in Fig. 10 were obtained 40 days later than the A traces. In the meantime, all samples were kept in pierced vials at room temperature. The non-homogeneity and instability of both Form II and Form III were evidenced in comparison to the stable Form I.

Solvates (and hydrates) are distinguished from polymorphs by the combination of DSC and TG applied to the

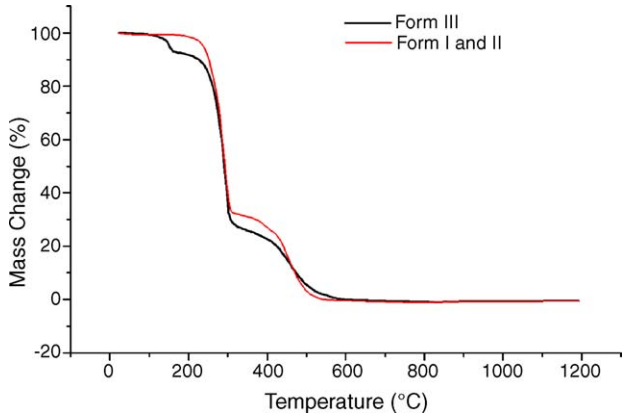

Fig. 11. TG curves of the MH forms. The curves for the Form I and Form II are completely overlapped. DTA curves are not shown for sake of clarity.

desolvation process. TG analysis confirmed that Form I and Form II are non-solvate and have the same weight loss curves, while the Form III shows an initial step around 180 °C, relative to the loss of one ethanol molecule (8% weight loss, Fig. 11).

4. Conclusions

Mepivacaine hydrochloride is official in USP 28th and European Pharmacopoeia 5th; a polymorphism is not reported. FT-IR spectroscopy, thermal analysis, single crystal and powder X-ray diffraction enabled us to identify and characterize different forms of MH in the solid state. Polymorphs are clearly differentiated by FT-IR, XRPD and HyperDSC not by conventional DSC. MH exists in at least two non-solvate forms (Form I and Form II) and one solvate form (Form III, emiethanolic solvate). More solvate forms may exist in equilibrium with the corresponding saturated solutions: a methanol solvate crystal was indeed grown in a capillary tube. Form III, the emiethanolic solvate, was obtained by re-crystallization from an ethanol 25% (w/v) solution, centrifugation and then drying at 50 °C in a vacuum dessiccator. By crystallization from various solvents at ambient conditions, Form I was always obtained. Form I is thermodynamically stable over the entire temperature range below its melting point with decomposition. Form II, present in commercial products, is metastable and can only be obtained by desolvation of the emiethanolic solvate. Industrial processing conditions, i.e. re-crystallization from ethanolic solutions at elevated temperatures and under vacuum, are likely to produce this transformation. The irreversible transformation to Form I occurs in few minutes at temperatures above 200 °C, and more important at ambient temperature in high relative humidity. Caking and aggregation can be observed when the stable form is attained at storage conditions. The presence of water is crucial for the phase transformations. The formation of the ethanolic solvate, and desolvate, is only possible

in the absence of or with very low water activity. Form II is kinetically stable for very long time in airtight containers. This polymorph, mostly present in commercial products due to the current industrial process of final drying, may be suitable for drug production. Since MH is a readily soluble drug compound, the existence of polymorphism has no relevance to its typical clinical use as water-dissolved active substance. The present study confirms the potential of ATR FT-IR as a quick, easy and cheaper alternative to XRPD [24]; the technique is ideally suited for polymorph analysis, because it is precise, accurate and requires minimal sample preparation.

Acknowledgements

The Authors thanks Dr. Maria Garavaglia (Perkin-Elmer, Italy) for HyperDSC analysis. Financial support from the Italian Ministero dell'Istruzione, dell'Università e della Ricerca is acknowledged.

References

[1] S. Datta, D.J.W. Grant, Nat. Rev. Drug Discovery 3 (2004) 42–57.
[2] S.R. Vippagunta, H.G. Brittain, D.J.W. Grant, Adv. Drug Deliv. Rev. 48 (2001) 3–26.
[3] D. Giron, Thermochim. Acta 248 (1995) 1–59.
[4] H.G. Brittain, E.F. Fiese, in: H.G. Brittain (Ed.), Polymorphism in Pharmaceutical Solids, vol. 95, Marcel Dekker, New York, 1999, pp. 331–361.
[5] D.E. Bugay, Adv. Drug Deliv. Rev. 48 (2001) 43–65.
[6] Csöeregh, Acta Cryst. Sec. C: Cryst. Struct. Commun. C48 (1992) 1794–1798.
[7] M. Bambagiotti-Alberti, B. Bruni, M. Di Vaira, V. Giannellini, Acta Cryst. E61 (2005) o585–o586.
[8] O.R. Sammul, W.L. Brannon, A.L. Hayden, J. Assoc. Off. Agric. Chem. 47 (1964) 918–991.
[9] http://www.aist.go.jp/RIODB/SDBS.
[10] S. Cherkaoui, J.L. Veuthey, J. Pharm. Biomed. Anal. 27 (2002) 129–136.
[11] M. Silaveru, J.T. Stewart, J. Pharm. Biomed. Anal. 15 (1997) 1751–1756.
[12] T.B. Vree, E.M. Beumer, A.J. Lagerwerf, M.A. Simon, M.J. Gielen, Anesth. Analg. 75 (1992) 75–80.
[13] M. Longobardo, E. Delpón, R. Caballero, J. Tamargo, C. Valenzuela, Mol. Pharm. 54 (1998) 162–169.
[14] B.F. Tullar, J. Med. Chem. 14 (1971) 891–892.
[15] C. Schmidt, V. Niederwanger, U.J. Griesser, J. Therm. Anal. Cal. 77 (2004) 639–652.
[16] M. Kuhnert-Brandstätter, A. Kofler, G. Kramer, Sci. Pharm. 42 (1974) 150–163.
[17] G.M. Sheldrick (Ed.), SADABS, Program for Empirical Absorption Corrections, University of Göttingen, Germany, 1986.
[18] A. Altomare, M.C. Burla, M. Camalli, G.L. Cascarano, C. Giacovazzo, A. Guagliardi, A.G.G. Moliterni, G. Polidori, R. Spagna, J. Appl. Cryst. 32 (1999) 115–119.
[19] G.M. Sheldrick, SHELXL-97, Program for Crystal Structure Refinement, University of Göttingen, 1997.
[20] L.J. Farrugia, J. Appl. Cryst. 30 (1997) 565.
[21] D.L. Bish, S.A. Howard, J. Appl. Crystallogr. 21 (1998) 86–91.
[22] A.C. Larson, R.B. von Dreele, Generalized Crystal Structure Analysis System, Los Alamos National Laboratory, NM, 2001.
[23] R.J. Hill, C.J. Howard, J. Appl. Cryst. 20 (1987) 467–474.
[24] R. Helmy, G.X. Zhou, Y.W. Chen, L. Crocker, T. Wang, R.M. Wenslow Jr., A. Vailaya, Anal. Chem. 75 (2003) 605–611.